Superalloys 2016: Proceedings of the 13th International Symposium on Superalloys
Edited by: Mark Hardy, Eric Huron, Uwe Glatzel, Brian Griffin, Beth Lewis, Cathie Rae, Venkat Seetharaman, and Sammy Tin
TMS (The Minerals, Metals & Materials Society), 2016

DEVELOPMENT OF NICKEL-COBALT BASE P/M SUPERALLOYS FOR DISK APPLICATIONS

Y. F. Gu[1], T. Osada[1], T. Yokokawa[1], H. Harada[1], J. Fujioka[1]
D. Nagahama[2], M. Okuno[2]

[1] National Institute for Materials Science (NIMS); 1-2-1 Sengen, Tsukuba-shi, Ibaraki, 305-0047 Japan
[2] Honda R&D Co., Ltd. Aircraft Engine R&D Center; 1-4-1 Chuo, Wako-shi, Saitama, 351-0193 Japan

Keywords: Ni-Co base superalloy, Disk, Powder metallurgy, Mechanical property

Abstract

A new generation of powder metallurgy (P/M) Ni-Co-base superalloys has been developed to allow rim temperatures in turbine disk beyond 700 °C. In a series of the alloys designed, nickel was substituted by cobalt in various proportions in some commercial Ni-base disk superalloys and cobalt content was ranging from 25 to 29 wt.%. Hot isostatic pressing (HIP) bars of new design alloys were manufactured for microstructure and property evaluation. Results from the mechanical properties assessment indicate that some new design alloys have at least 69 °C temperature advantage in 0.2%-strain creep performance, higher tensile strength, comparable low-cycle fatigue (LCF) life, phase stability and oxidation resistance compared with P/M alloy 720Li.

Introduction

The operating temperature for the rim sections (near the gas flow path) of high-pressure turbine disk has continued to increase as the turbine inlet temperature increases, which presents a challenge to materials researchers. To achieve a temperature capability beyond 700 °C for use in high-pressure turbine disks of modern aero-engines, a new generation of high-performance P/M superalloys has been developed by a collaborative project initiated by the NIMS and Honda R&D Co., Ltd. from April 2008 to March 2011. The required characteristics for mechanical properties of the P/M superalloys were high tensile strength, high creep resistance and LCF life associated with a suitable damage tolerance capability up to 750 °C. The objective of the initial development phase was to design compositions based on combining the characters of two kinds of γ–γ′ two-phase (Ni-base and Co-base alloys) and maintaining γ–γ′ two-phase structure with high Co and Ti contents [1-5], evaluate experimental alloy compositions in laboratory screening trials in terms of microstructure and property assessment, and manufacture hot isostatic pressing (HIP) bars and hot-extruded bars for additional microstructure and property assessments. The outcome of this collaborative project was a new kind of patented P/M superalloy based on Ni-Co matrix and containing 46-55% γ′-fraction strengthening precipitates with an enhanced balance of tensile strength, low-cycle fatigue (LCF) life, creep and oxidation resistance properties [6]. The paper report herein focuses on overall alloy development methodology including alloy design strategy, microstructure, initial tensile and creep results of heat-treated P/M Ni-Co-base superalloys compared with the properties of P/M alloy 720Li, RR1000 and ME3 alloys reported [7-10].

Materials and Experimental Procedures

The P/M superalloys were designed by an original concept validated for TMW alloys (**T**okyo **M**eguro or **T**sukuba **M**aterial Cast & **W**rought (C&W) superalloy) [1-5], designated as TMP (**T**okyo **M**eguro or **T**sukuba **M**aterial **P**owder metallurgy superalloy) or HGN alloy (code name of Honda R&D) [6]. Figure 1 shows a schematic illustration of the alloy design concept for Ni-Co base P/M superalloys based on a combination of Ni base superalloys and Co base alloys both with γ/γ′ two-phase structure. First, an equilibrium phase calculation program with a Ni-database7 (Thermo-Calc Software, Sweden) was used to predict the existence of stable phases in designed TMP (HGN) alloys, and then the microstructure and compression properties were investigated by samples from small arc-melted ingots.

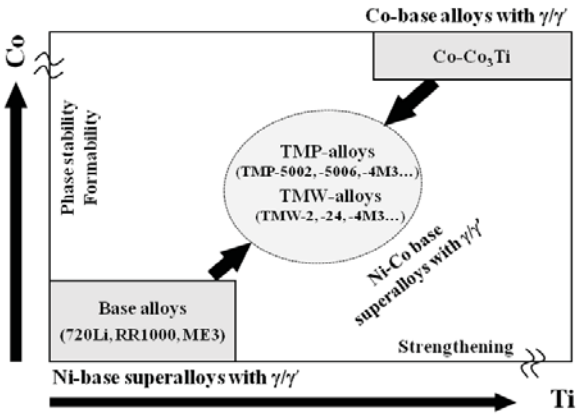

Figure 1. Alloy design concept of Ni-Co base superalloy for P/M disks.

The typical compositions of the alloys designed, along with the volume fraction of γ′ phase, γ′ solvus temperature and long term aging test results are listed in Table I and II where #400X, #500X and #10X were designed based on the combination of Co-Ti base alloys with RR1000 [7, 9-10], ME3 [8] and 720Li alloys, respectively. The TMP (HGN) alloys normally have a Co content of 25 to 29 wt.%, a Ti content of 3.9 to 6.2 wt.% and a volume fraction of 46% to 55%. Some of the TMP (HGN) alloys designed were used for additional screening based on the results of investigations of microstructure stability and mechanical properties.

Material for additional screening was prepared by the normal P/M processing route. Alloy powders prepared by argon gas atomization and passed through screens of -160 mesh to give powder particle diameters of no more than about 100 μm were

Table I. Nominal Compositions of P/M Alloys Tested (in Weight ercent)

Alloy	Remarks	Cr	Co	Mo	W	Ti	Al	C	B	Zr	Ta	Hf	Nb	Ni
#101	720Li	16.0	15.0	3.0	1.3	5.0	2.5	0.03	0.02	0.03	-	-	-	Bal.
#102	TMW-2	14.4	21.8	2.7	1.1	6.2	2.3	0.03	0.02	0.03	-	-	-	Bal.
#103	TMW-24	13.8	25.0	2.6	1.1	5.6	2.2	0.03	0.02	0.03	-	-	-	Bal.
#104	TMW-4	14.9	26.2	2.8	1.1	6.1	1.9	0.02	0.02	0.03	-	-	-	Bal.
#105	TMW-4M3	13.5	25.0	2.8	1.2	6.2	2.3	0.03	0.02	0.03	-	-	-	Bal.
#4002	TMP (HGN)	14.3	25.0	4.8	0.0	4.0	2.9	0.025	0.02	0.05	2.5	0.7	-	Bal.
#4003	TMP (HGN)	13.5	25.0	4.5	0.0	4.4	2.7	0.025	0.02	0.05	1.8	0.7	-	Bal.
#4004	TMP (HGN)	13.5	25.0	4.5	0.0	4.4	2.7	0.025	0.02	0.05	1.8	0.35	-	Bal.
#4006	TMP (HGN)	12.7	25.0	4.2	0.0	5.0	3.0	0.025	0.02	0.05	2.1	0.7	-	Bal.
#5001	TMP (HGN)	11.7	25.0	3.4	1.9	4.2	3.2	0.025	0.02	0.05	2.2	0.35	0.8	Bal.
#5002	TMP (HGN)	11.7	27.0	3.4	1.9	4.4	3.2	0.025	0.02	0.05	2.2	0.35	0.5	Bal.
#5003	TMP (HGN)	12.5	27.0	3.4	1.9	4.4	3.2	0.025	0.02	0.05	2.5	0.35	0.5	Bal.
#5004	TMP (HGN)	12.5	25.0	4.5	2.1	4.4	3.2	0.025	0.02	0.05	2.5	0.35	0.5	Bal.
#5006	TMP (HGN)	11.7	29.0	3.7	2.1	3.9	2.9	0.025	0.02	0.05	2.1	0.35	0.5	Bal.

Table II. Typical Characters of P/M Alloys Tested

Alloy	Ti/Al Ratio	Calculated volume fraction of γ' V_f	Calculated γ' solvus $T(^oC)$	Long time aging TCP phase*	Corresponding C&W alloy
#101	2.0	45	1154	0	U720Li
#102	2.7	48.5	1190	0	TMW-2
#103	2.5	46	1166	0	TMW-24
#104	3.2	45	1126	0	TMW-4
#105	2.7	50.5	1180	0	TMW-4M3
#4002	1.4	48	1151	xx	-
#4003	1.6	47	1158	0	-
#4004	1.6	46	1155	0	-
#4006	1.7	53	1186	x	-
#5001	1.3	53	1174	0	-
#5002	1.4	54	1180	0	-
#5003	1.4	54	1176	xx	-
#5004	1.4	55	1174	xxx	-
#5006	1.3	47.5	1147	0	-

* No TCP phase (0), low amount of TCP phase (x), not acceptable for the application (xx or xxx)

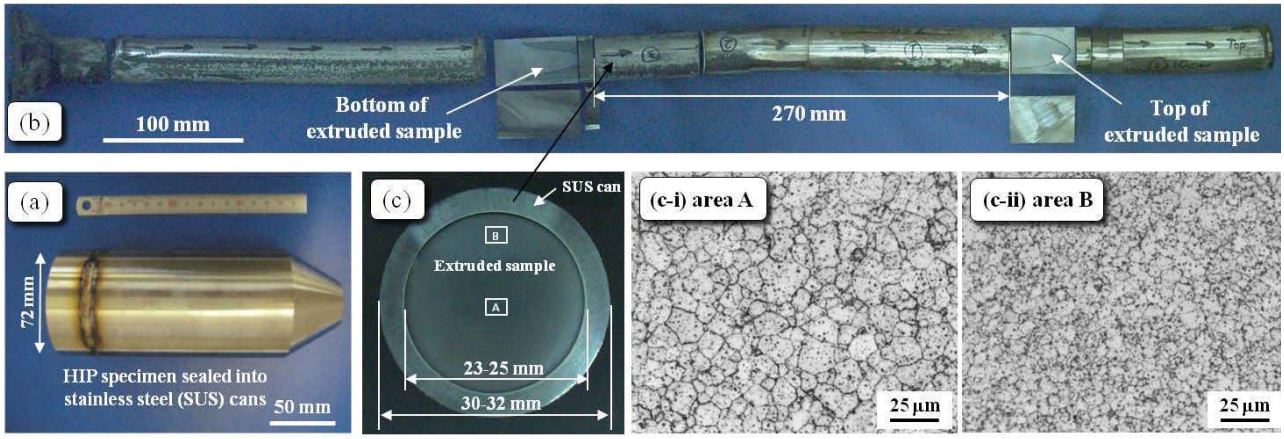

Figure 2. Typical images of extruded bar and microstructure: (a) sealed HIP alloy, (b) extruded bar and(c) microstructures of extruded bar, the area A (c-i) and the area B (c-ii) in (c).

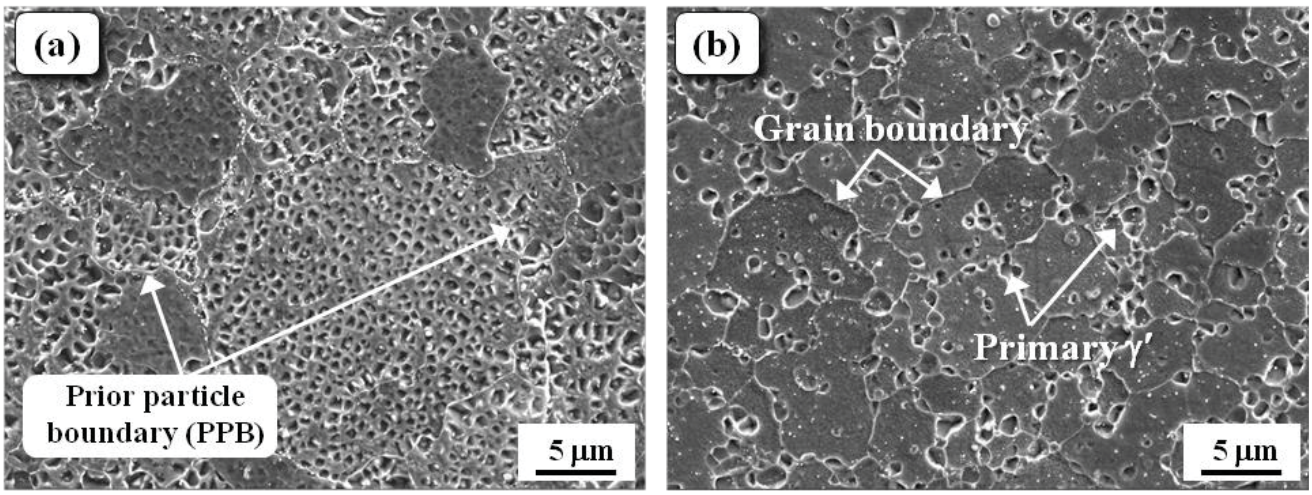

Figure 3. Secondary electron images of microstructure in (a) HIP sample and (b) extruded bar.

sealed into cans and subsequently formed by HIP into 150 mm in diameter and 300 mm in length bars, and then hot-extruded into 25 mm in diameter bars to reduce the effect of prior particle boundaries (PPBs) phase in P/M products as shown in Figure 2. The grain sizes varied from 5 μm to 30 μm in the as-HIPed samples, and were minimized to about 3 μm to 5 μm in the outer area of the extruded bar while the PPBs were reduced after hot extrusion as shown in Figure 3. The tensile and creep specimens were taken from the HIP bar, and the LCF specimens were taken from the outer area of the extruded bars. Then, all samples were heat treated at a solution temperature from 1100～1150 °C for 4 h then air cooled, primary aged at 650 °C for 24 h then air cooled and secondary aged at 760 °C for 16 h then air cooled.

Prior to mechanical testing, the initial microstructures of the heat-treated HIP and extruded specimens were characterized by the analysis techniques of optical microscope and a field emission scanning electron microscope (FE-SEM, JEOL JSM-7001F) with electron backscatter diffraction (EBSD). The specimens were prepared by metallographic polishing. For optical microscope observation, the polished specimens were etched in a solution of Kalling reagent (25 g $CuCl_2$ + 50 ml HCl + 50 ml H_2O). EBSD was carried out in the FE-SEM operating at 15 kV using the TSL OIM data collection program. The average value of grain size and ASTM grain size number of grain boundary excluding annealing twin boundary were measured from the EBSD data using the TSL OIM analysis program.

Tensile specimens were tested at temperatures ranging from room temperature to 800 °C. Constant load tensile creep rupture tests were conducted at 650 °C and 830 MPa, 725 °C and 630 MPa, and 760 °C and 480 MPa. Additionally, LCF test specimens with a gauge section of 4 mm in diameter and 13.5 mm in length were cut from the heat-treated extruded bars. The LCF tests were conducted at 650 °C with a triangle waveform and total strain range $\Delta\varepsilon_t$ of 0.8, 1.0 and 1.2% under strain control conditions ($R\varepsilon_t = \varepsilon_{min}/\varepsilon_{max} = 0$). The fracture initiation site on the fracture surface after LCF tests was identified using FE-SEM with energy dispersive x-ray spectroscopy (EDS).

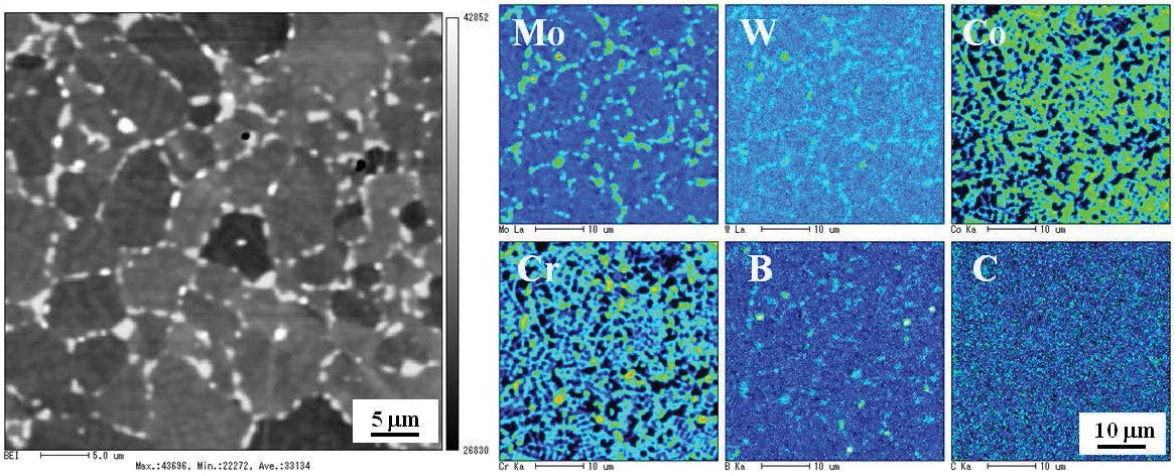

***Yellow and Green=high concentration; Blue=low concentration; Black = no concentration**

Figure 4. Backscattered electron image (left) and images from electron probe micro-analyzes of the HIP #5004 alloy exposed at 850 °C for 5000 hours.

For the thermal phase stability and isothermal oxidation tests, the heat-treated HIP bars were cut into cylindrical shape 5 mm in height and 9 mm in diameter. Their surfaces were finally polished by #1000 SiC paper. The isothermal oxidation tests were conducted at 650 °C, 750 °C and 850 °C up to 5000 hours. The weight of the sample was measured after oxidation. The phase constitutions and the microstructure stability of the samples after thermal exposure at 650 °C, 750 °C and 850 °C from 1000 to 5000 hours were investigated by electron probe micro-analyzer (EPMA, Shimadzu-1610).

Results and Discussion

Microstructure and Thermal Stability

The compositions and microstructure investigation results of the alloys tested (#10X, #400X and #500X) and subjected to heat treatment and thermal exposure are indicated in Table I and Table II. Ten of the alloys tested had only a γ/γ′ two-phase structure with no topologically closed packed (TCP) phases such as μ and σ phase (0 in Table II) after heat treatment and long-term exposure at high temperature (5000 hours at 650 °C, 750 °C and 850 °C). The alloy #4006 had low amounts of TCP phases (x in Table II), and the alloys #4002, #5003 and #5004 had unacceptable amounts of TCP phases (xx or xxx in Table II) for the disk applications.

Figure 4 shows the images and compositions measured by EPMA in the HIP #5004 alloy exposed at 850 °C for 5000 hours. In the HIP #5004 alloy, $(Mo, W)_x(B, C)_y$ phase and $(Cr, Mo)_x(Ni, Co)_y$ phase (σ-phase) existed at grain boundaries and within the grains in addition to the γ and γ′phases.

Tensile Properties

Tensile tests of the heat-treated HIP alloys were conducted from room temperature (20 °C) to 800 °C. The temperature dependence of the ultimate tensile strength (UTS) and elongation (EL) is shown in Figure 5. At room temperature, the UTS value of P/M 720Li (#101) alloy was 1634 MPa and all other designed alloys showed UTS values greater than 1700 MPa. At 800 °C, the UTS values of the alloys designed were about 100 MPa higher than that of P/M 720Li (#101) alloy and are comparable with the value of ME3 from a supersolvus solution heat treatment [8]. Alloy #5004 had better combined tensile properties compared with P/M 720Li (#101), ME3 and Alloy #5006, due to its higher γ′ volume fraction.

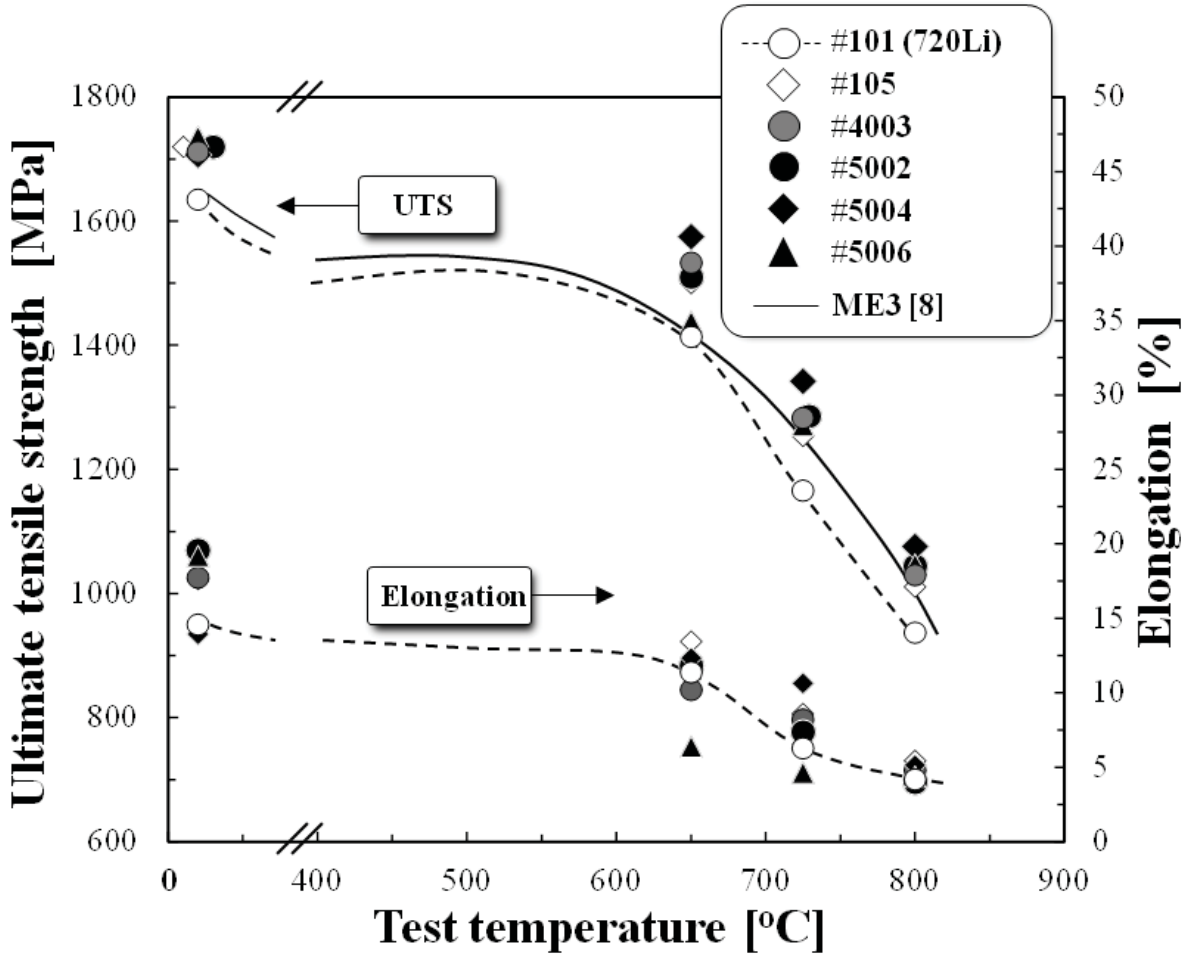

Figure 5. Temperature dependence of ultimate tensile strength and elongation of the heat-treated HIP alloys prepared via P/M processing route.

Creep-Rupture Properties

Tensile creep tests of heat-treated HIP alloys with 10 μm average grain size have been performed in air under the load range from 480 MPa to 830 MPa and in the temperature range from 650 °C to 760 °C where the alloys are to be used. The results from these tests are shown in Figure 6. The temperature capability for 0.2%-creep strain as estimated from the Larson Miller Parameter (LMP) by use of c = 20 showed a 100-hour life increase with the addition of Co-Co_3Ti, such as #105 corresponding to TMW-4M3 [1-5], #5002 and #5006 alloys (Figure 6(a)). The temperature capability of alloys #105, #5002 and #5006 was estimated to be 743 °C, 741 °C and 740 °C, which were 72 °C, 70 °C and 69 °C higher than that of P/M 720Li (#101), respectively (Figure 6(b)). Furthermore,

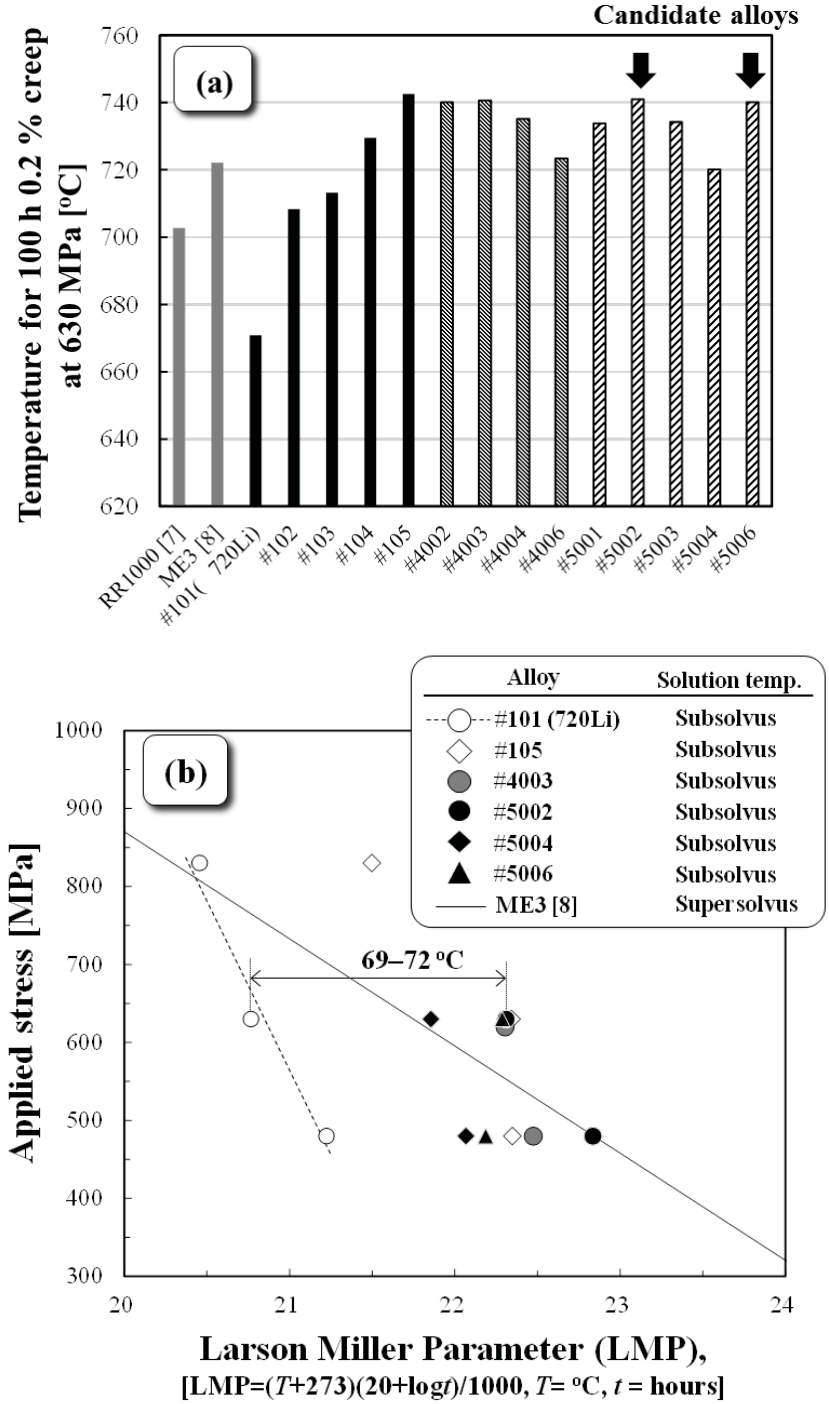

Figure 6. (a) Temperature capabilities for 0.2%-creep-strain life at 630 MPa for 100 hours; (b) Larson-Miller plot of 0.2 % creep life for HIP alloys prepared via P/M processing route.

some TMP (HGN) alloys have better creep resistance than that of ME3 above 600 MPa, but lower than that of ME3 below 600 MPa because TMP alloys are subsolvus solution heat treated and have finer grain size to that shown by ME3 alloy, heat-treated at a supersolvus temperature (G7.1, ASTM grain size number) [8]. It was reported that the creep life of TMW-4M3 significantly improves with increasing grain size in the lower stress region [4]. Therefore, the optimization of microstructure including factors such as primary, secondary and tertiary γ' precipitates together with coarsening the grain size may improve the creep properties of TMP (HGN) alloys.

LCF Properties

The LCF life of the extruded P/M alloys at 650 °C is shown as a function of strain range in Figure 7a. The data plots attached with asterisks indicate the specimens fractured from embedded flaw. Meanwhile, average LCF life of conventional C&W U720Li [4] obtained at the similar test temperature range was used as a comparison. For all of the P/M alloys tested, the LCF life was almost the same and some designed alloys had slightly shorter values than the average life for C&W U720Li. Furthermore, amongst the tested alloys, the LCF life of #5002 shows the best

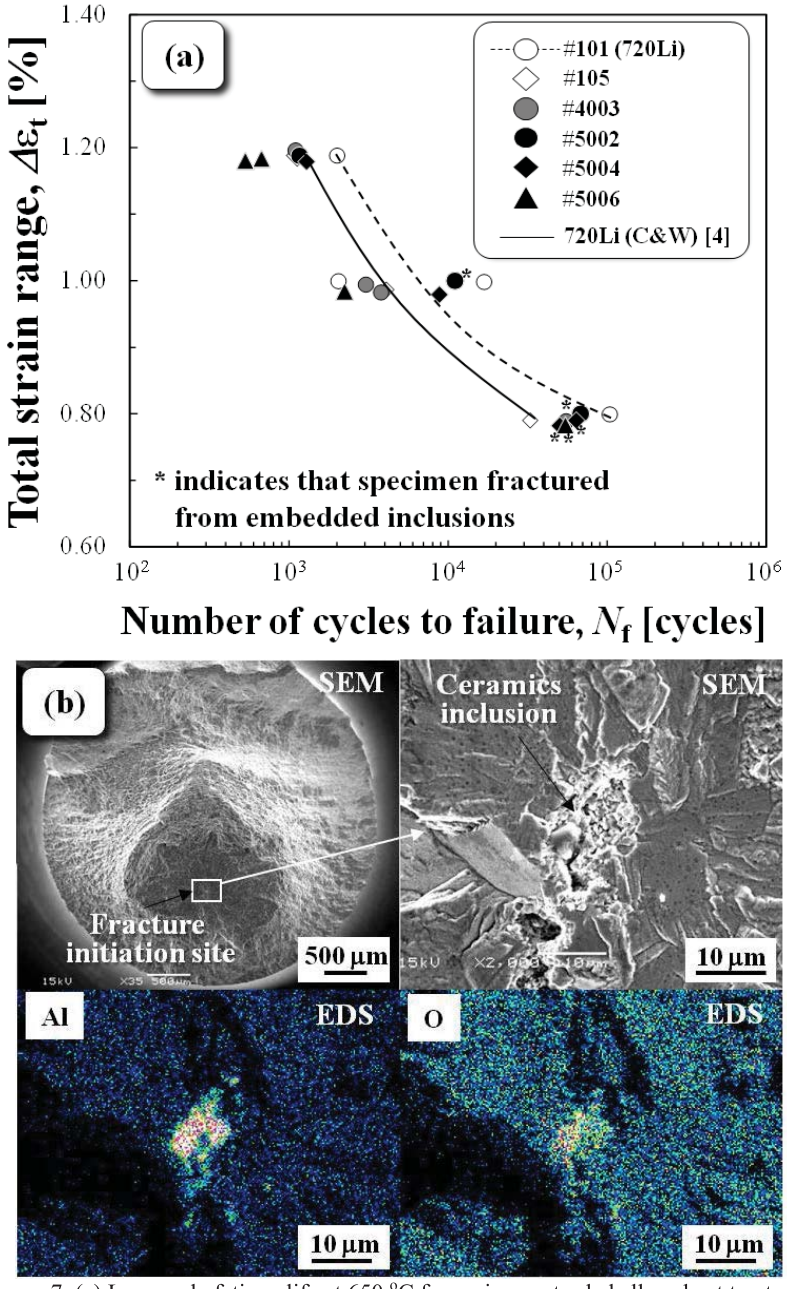

Figure 7. (a) Low cycle fatigue life at 650 °C for various extruded alloys heat treated at subsolvus temperature, (b) fracture initiation site and EDS maps of the #5006 alloy tested at $\Delta\varepsilon_t$ =0.8%.

value compared with the other designed alloys. For most of #500X alloys, fatigue failures tended to occur at internal crack initiation sites (embedded flaw in Figure 7b) for low strains ($\Delta\varepsilon_t$= 0.8%). The embedded flaws identified by EDS analysis were the ceramic inclusions mainly composed of metals Al and O in #400X and #500X HIP bars. But, similar ceramic inclusions were not observed in #10X alloys.

Oxidation resistance

For applications beyond 700 °C, good oxidation resistance of turbine disk superalloys is also required. Isothermal oxidation tests of heat-treated HIP specimens were carried out at 650 °C, 750 °C and 850 °C up to 5000 hours. For all test temperatures and all developed alloys, weight gain in mg/cm^2, Δw, followed the

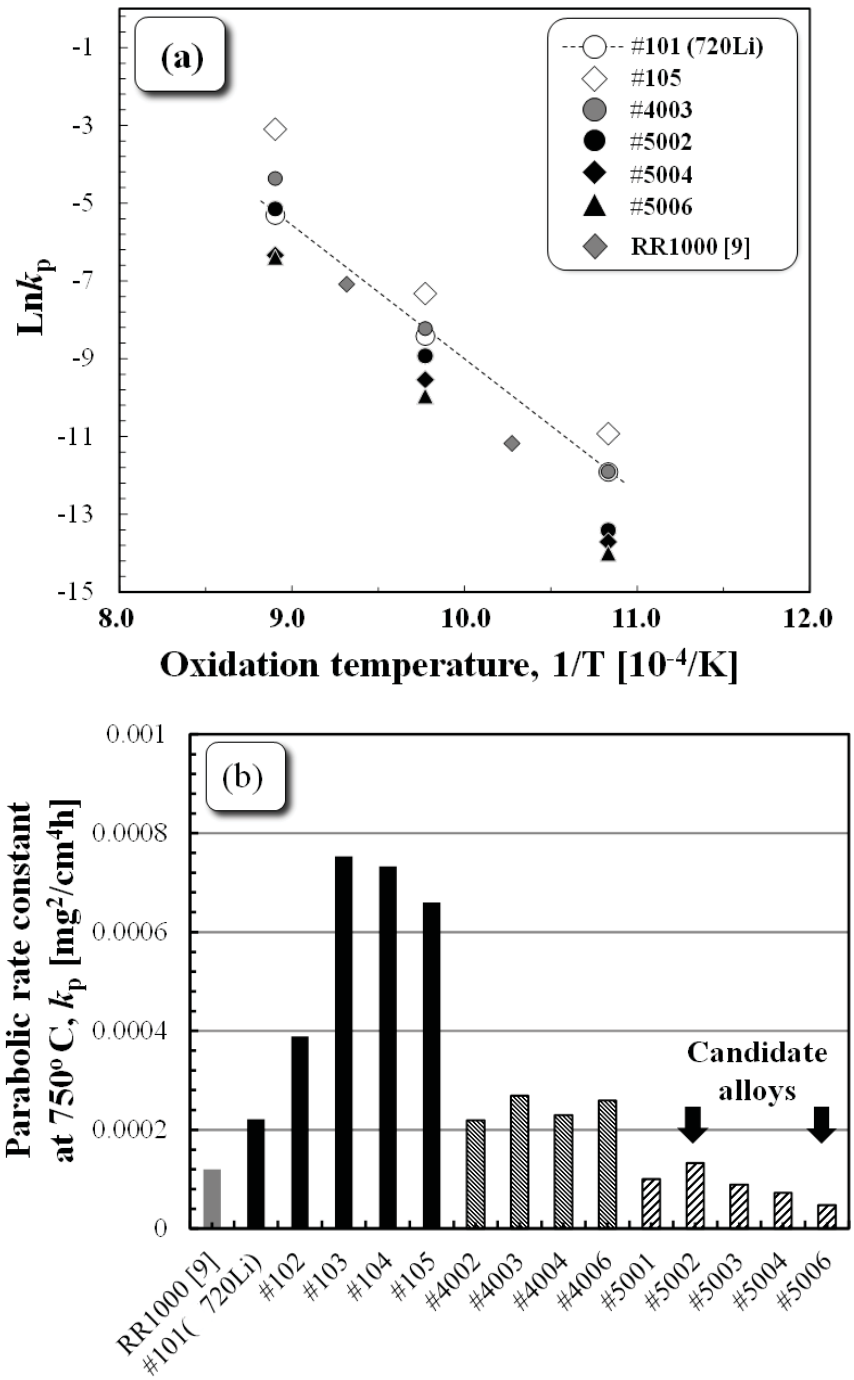

Figure 8. (a) Arrhenius plot indicating the temperature dependence on parabolic rate constant, k_p, and (b) the values of k_p at 750 ^{o}C of the HIP alloys heat-treated subsolvus temperature.

Wagner's parabolic growth model given by:

$$\Delta w^2 = k_p t \quad (1)$$

where k_p is a parabolic rate constant in mg^2/cm^4h and t is a exposure time in hours. Results suggest that oxide growth follows the diffusion-controlled growth for the oxidation of the tested alloys. Thus, the temperature dependence on k_p was evaluated by using Arrhenius plot given by:

$$k_p = k_o \exp\left(\frac{-E_A}{RT}\right) \quad (2)$$

where k_o is a frequency factor, E_A is the activation energy for oxidation, R is a gas constant and T is a exposure temperature. As shown in Figure 8a, the $\ln k_p$ is proportional to 1/T with almost the same slopes for all alloys tested and in good agreement with the equation (2), where E_A value varied from 284 kJ/mol to 386 kJ/mol and average E_A value for all P/M alloys tested was 326 kJ/mol. The average value is almost the same or slightly higher than that for conventional Ni-base disk superalloy [10]. Figure 8b shows the k_p at 750 °C for P/M alloys tested. For comparison, the reported data for RR1000 [9] is also shown alongside. As shown in the Figure 8b, #5002 and #5006 alloys exhibit the lowest k_p, indicating excellent oxidation resistance.

Conclusions

A new kind of P/M disk superalloy, named TMP (HGN) alloy, was proposed and developed in collaborative research between NIMS and HONDA R&D Co., Ltd.. The evaluation of mechanical properties from HIPed and hot-extruded bars indicate that #5002 (named TMP5002 or HGN200) and #5006 (named TMP5006 or HGN300) alloys exhibit superior thermal phase stability, oxidation resistance and 100 MPa higher ultimate tensile strength compared with P/M 720Li up to 800 °C. Meanwhile, TMP5002 (HGN200) and TMP5006 (HGN300) provide at least 69 °C temperature advantage in 0.2%-strain creep performance compared with the P/M 720Li alloy. These results indicate that some TMP (HGN) alloys are good candidates for turbine disk applications beyond 700 °C.

References

1. Y.F. Gu et al., "New Ni-Co-base Disk Superalloys with Higher Strength and Creep Resistance", *Scripta Materialia*, 55 (2006), 815-818.

2. Y.F. Gu et al., "Comparison of Mechanical Properties of TMW Alloys, New Generation of Cast-and-Wrought Superalloys for Disk Applications", *Metall. Mater. Trans. A*, 40A (2009), 3047-3050.

3. Y. Yuan et al., "A Novel Strategy for the Design of Advanced Engineering Alloys-Strengthening Turbine Disk Superalloys via Twinning Structures", *Adv. Engng. Mater.*, 13 (2011) , 296-300.

4. J Fujioka et al., "Development of Ni-Co-base Superalloys Based on New Concept for High Temperature Turbine Disk Applications", *Proceedings of Inter. Gas Turbine Congress 2015 Tokyo* (Minatoku, Tokyo, Gas Turbine Society of Japan, 2015), 333-338.

5. T. Osada et al., "Optimum Microstructure Combination in a Polycrystalline Superalloy with Two-Phase Structure", *Acta Mater.* 61 (5) (2013), 1820-1829.

6. Y.F. GU et al., "Nickel alloy", patent US8,961,646,B2 (2015).

7. A. Banik et al., "Low Cost Powder Metal Turbine Components", *Superalloys 2004,* ed. K.A. Green et al. (Warrendale, PA: TMS 2004), 571-576.

8. T.P. Gabb et al., "Characterization of the Temperature Capabilities of Advanced Disk Alloy ME3" (Report NASA/TM 2002-211796, NASA Glenn Research Center, 2002).

9. A. Encinas-Oropesa et al., "Evaluation of Oxidation Related Damage Caused to a Gas Turbine Disk Alloy Between 700 and 800 °C", *Materials at High Temperatures*, 26(3) (2009), 241-249.

10. A. Encinas-Oropesa et al., "Effect of Oxidation and Hot Corrosion in a Nickel Disk Alloy", *Superalloys 2008*, ed. R.C. Reed et al. (Warrendale, PA: TMS 2008), 609-618.